Research Square

Preprints are preliminary reports that have not undergone peer review.
They should not be considered conclusive, used to inform clinical practice,
or referenced by the media as validated information.

Electronic Effects on the ESIPT and Antioxidant Activity of the Dihydrochalcone Phloretin

Zhongxin Zhang
Xinjiang Normal University
XinTian Song
Xinjiang Normal University
Reyihanguli Tudi
Xinjiang Normal University
Abulimiti Yasen
Xinjiang Normal University
Jiaqi Li
Xinjiang Normal University
Xiaoning Wang
Xinjiang Normal University
Mei Xiang
mei811014@126.com
Xinjiang Normal University
Bumaliya Abulimiti
Xinjiang Normal University

Research Article

Keywords: Phloretin, ESIPT, antioxidant activity, functional group modification, density functional theory (DFT)

Posted Date: April 11th, 2026

DOI: https://doi.org/10.21203/rs.3.rs-9060282/v1

License: This work is licensed under a Creative Commons Attribution 4.0 International License.
Read Full License

Additional Declarations: No competing interests reported.

Abstract

Context

A dynamic balance between oxidation and antioxidation is essential for maintaining normal physiological functions in the human body. Disruption of this balance, resulting from insufficient antioxidant capacity, leads to oxidative stress and subsequent cellular damage. Phloretin (PHL), a naturally occurring dihydrochalcone, exhibits distinctive antioxidant activity that is closely linked to its excited-state intramolecular proton transfer (ESIPT) characteristics. Despite its potential, the systematic influence of substituent modifications on the ESIPT process and the resulting antioxidant activity remains largely unexplored. In this study, we designed six novel PHL derivatives by introducing electron-donating groups (-OH, -NH_2, -CH_3) and electron-withdrawing groups (-CN, -NO_2, -CHO) to elucidate the regulatory effects of these functional groups on the ESIPT mechanism and antioxidant performance. Using density functional theory (DFT) and time-dependent DFT (TD-DFT), we systematically investigated the geometric structures, infrared spectra, reduced density gradient, molecular orbitals, potential energy curves, and antioxidant activities of PHL and its derivatives. Our results reveal that while pristine phloretin lacks an E* state during its ESIPT process, the incorporation of strong electron-withdrawing groups (-NO_2, -CHO) restores the typical four-state ESIPT pathway. Notably, electron-donating and electron-withdrawing groups exert opposing regulatory effects: the former facilitate the ESIPT process and substantially enhance antioxidant activity, whereas the latter suppress ESIPT and concurrently diminish antioxidant capacity. This work establishes a crucial theoretical foundation for the rational design of high-performance antioxidants through targeted functional group engineering to precisely modulate ESIPT and antioxidant activity.

Methods

All computational studies in this paper were performed using the Gaussian 16 software package (Revision B.01), while GaussView 6.0.16 was employed for the analysis and visualization of compounds. To identify the most suitable computational method for the phloretin system, four functionals—B3LYP, B3PW91, Cam-B3LYP, and PBE were evaluated by comparing calculated absorption maxima with experimental data. Based on this benchmark, ground-state (S_0) geometries were optimized using the B3LYP functional in conjunction with the TZVP basis set, while excited-state (S_1) optimizations were carried out using the long-range corrected Cam-B3LYP functional with the same basis set. Frequency analyses confirmed the absence of imaginary frequencies for all optimized structures, verifying that they correspond to genuine local minima on the potential energy surface. Solvent effects were modeled using the integral equation formalism of the polarizable continuum model (IEFPCM) to simulate a methanol environment. Antioxidant activity was assessed by calculating the ionization potential (IP). Post-processing analyses, including reduced density gradient (RDG) analysis and frontier molecular orbital (FMO) visualizations, were conducted using the Multiwfn 3.8 (dev) and VMD 1.9.3 software.

1. Introduction

Flavonoids, a class of natural bioactive molecules abundant in fruits and vegetables [1,2], exhibit antioxidant capacities that can help delay bodily aging processes [3,4]. Skin aging, a systemic physiological change, is directly linked to the decline in antioxidant defense. With advancing age, decreased efficiency in scavenging free radicals leads to the accumulation of oxidative stress, which in turn accelerates the deterioration of skin structure and function [5]. Consequently, enhancing antioxidant activity has emerged as a crucial strategy for combating skin aging. Notably, studies have demonstrated that modulating the excited-state intramolecular proton transfer (ESIPT) process in flavonoids through structural modification can effectively boost their antioxidant properties, providing a key rationale for designing potent antioxidant molecules [6,7].

As a representative dihydrochalcone within the flavonoid family [8,9], phloretin exhibits antioxidant activity that is intrinsically linked to its ESIPT process. Recent studies have further revealed that the antioxidant activity of flavonoid derivatives is markedly enhanced in the excited state (S_1), with this enhancement being directly correlated with ESIPT efficiency [10]. Although a higher number of hydroxyl groups is typically associated with greater antioxidant capacity [11], the structural modification space is often limited. This raises a key scientific question: how can the ESIPT process be precisely modulated through targeted functional group introduction to maximize antioxidant efficiency? Addressing this question is crucial not only for elucidating the antioxidant mechanisms of flavonoids but also for providing a theoretical foundation for developing novel agents against oxidative stress-related skin aging.

Investigating the excited-state intramolecular proton transfer (ESIPT) process is crucial for elucidating how functional groups influence the physicochemical properties of organic molecules [12–14]. ESIPT involves the photoexcitation-induced migration of a proton from a hydrogen-bond donor to an adjacent acceptor group, leading to molecular isomerization. Notably, not all molecules exhibit such photo-induced isomers. This study focuses on phloretin, which, despite possessing S_1-state isomers, does not exhibit the characteristic E* state in its ESIPT process. Intriguingly, introducing strong electron-withdrawing groups (-NO_2 and -CHO) into its structure results in derivatives that display a complete four-state ESIPT mechanism [15–17]. To our knowledge, such a regulatory phenomenon has not been previously reported, underscoring the significance of systematically exploring the effects of functional group modification on both the ESIPT pathway and antioxidant activity.

In this study, we systematically designed six phloretin derivatives by introducing electron-donating and electron-withdrawing groups. Utilizing density functional theory (DFT) and time-dependent DFT (TD-DFT), we investigated the regulatory mechanism of these functional group substitutions on the excited-state intramolecular proton transfer (ESIPT) process and antioxidant activity [18]. A comprehensive analysis was conducted, including geometric parameters (bond lengths and angles), infrared (IR) spectroscopy, non-covalent interactions (NCI), frontier molecular orbitals (FMOs), absorption and fluorescence spectra, and potential energy curves (PECs) [19], to elucidate the ESIPT process. Concurrently, the antioxidant

capacity was evaluated by calculating the ionization potential (IP). This work establishes a theoretical framework for designing more potent antioxidants.

2. Method of calculation

The ESIPT process and antioxidant activity of phloretin and its derivatives in both ground and excited states were comprehensively investigated using DFT and TD-DFT [20]. To identify the most suitable computational method, we evaluated four functionals (B3LYP, B3PW91, Cam-B3LYP, PBE) for calculating the absorption peaks of phloretin and its derivatives, benchmarking the results against experimental data in Table 1 [21]. Based on this assessment, the ground-state (S_0) geometries were optimized at the B3LYP/TZVP level, while the excited-state (S_1) optimizations employed the long-range corrected Cam-B3LYP functional with the same basis set [22]. Frequency analyses confirmed the absence of imaginary frequencies for all optimized structures, verifying that they represent true local minima on the potential energy surface [23]. All calculations utilized the integral equation formalism variant of the polarizable continuum model (IEFPCM) to simulate a methanol solvent environment. Furthermore, to map the ESIPT pathway, potential energy curves (PECs) for the ground and excited states were constructed by performing relaxed scans along the O1–H2 bond coordinate (16 steps, step size 0.05 Å). These PECs enabled the location of transition states and the calculation of energy barriers, providing direct insight into the feasibility of the proton transfer. Antioxidant activity was assessed via the calculation of the ionization potential (IP). All electronic structure computations were performed using the Gaussian 16 software package [24]. Post-processing analyses, including reduced density gradient (RDG) analyses and frontier molecular orbital (FMO) visualizations, were conducted with the Multiwfn-3.8 [25, 26] and VMD programs.

Table 1
Calculated Absorption Peaks (λmax) of Phloretin (PHL) Using Different Functionals

	B3LYP	B3PW91	Cam-B3LYP	PBEPBE	Exp
PHL	344.42nm	345.09nm	286.79nm	421.45nm	287.5nm

3. Results and discussion

3.1. Geometric Structures and Infrared Spectra

The intramolecular hydrogen bond (IMHB) is a prerequisite for the ESIPT process, and its geometric parameters, such as bond lengths and angles, are critical indicators [27]. As shown in Fig. 1, key atoms involved in ESIPT are numerically labeled. The corresponding bond lengths and angles for phloretin (PHL) and its derivatives in the S_0 and S_1 states are summarized in Table 2. A shorter IMHB length generally signifies a stronger interaction. In the S_0 state, the H2···O1 distance in pristine PHL is 1.5652 Å. With the introduction of electron-donating groups (-OH, -NH_2, -CH_3), this distance shortens further to 1.56359, 1.56452, and 1.56511 Å in PHL-OH, PHL-NH_2, and PHL-CH_3, respectively, suggesting a

promotion of the ESIPT process. Conversely, electron-withdrawing groups (-CN, -NO_2, -CHO) lead to elongated H2···O1 distances of 1.57051, 1.57023, and 1.56598 Å in PHL-CN, PHL-NO_2, and PHL-CHO, which would inhibit ESIPT compared to PHL. Furthermore, for most derivatives (PHL-OH, PHL-NH_2, PHL-CH_3, PHL-CN), the H2···O1 bond is shorter in the S_1 state than in the S_0 state, implying that ESIPT is more favorable upon photoexcitation. Interestingly, for PHL-NO_2 and PHL-CHO, the bond lengthens in the S_1 state, indicating that ESIPT becomes less likely compared to the ground state.

Table 2
Key Geometric Parameters (Bond Lengths in Å and Bond Angles in °) for the Intramolecular Hydrogen Bond in Phloretin (PHL) and Its Derivatives in Methanol Solution

	State	O_3-H_2	H_2…O_1	O_1-H_2…O_3
PHL	S_0	1.00177	1.56520	150.57068
	S_1	1.60142	0.99835	150.61947
PHL-OH	S_0	1.00210	1.56359	150.63816
	S_1	1.58743	0.99928	151.07275
PHL-NH_2	S_0	1.00191	1.56452	150.60852
	S_1	1.60039	0.99842	150.60957
PHL-CH_3	S_0	1.00177	1.56511	150.57197
	S_1	1.59927	0.99845	150.69636
PHL-CN	S_0	1.00079	1.57051	150.35925
	S_1	1.59829	0.99925	151.12244
PHL-NO_2	S_0	1.00081	1.57023	150.36684
	S_1	0.99547	1.57924	149.22761
PHL-CHO	S_0	1.00178	1.56598	150.56935
	S_1	0.99736	1.56911	149.68554

To further validate the geometric structures, the infrared (IR) absorption spectra of phloretin (PHL) and its derivatives in both S_0 and S_1 states were calculated [28], as shown in Fig. 2. Red-shifted and blue-shifted IR stretching frequencies are indicative of strengthened and weakened intramolecular hydrogen bonds (IMHBs), respectively. The O-H stretching frequency for the pristine PHL molecule is observed at 3046 cm^{-1}. Upon introducing electron-donating groups (-OH, -NH_2, -CH_3), the corresponding frequencies for PHL-OH, PHL-NH_2, and PHL-CH3 red-shift to 3039, 3041, and 3045 cm^{-1}, signaling a strengthening of

the IMHB. Conversely, derivatives with electron-withdrawing groups (-CN, -NO_2, -CHO)—PHL-CN, PHL-NO_2, and PHL-CHO—exhibit blue-shifted frequencies of 3063, 3062, and 3047 cm^{-1}, which point to a weakening of the IMHB. These spectral trends indirectly reflect the relative ease or difficulty of the ESIPT process. Crucially, the IR findings are fully consistent with the geometric parameter analysis (Table 2), mutually corroborating the reliability of our conclusions.

3.2 Non-covalent interaction analysis

The non-covalent interactions within the systems were visualized using the reduced density gradient (RDG) method, with the corresponding scatter plots presented in Fig. 3. In RDG analysis, the strength of a hydrogen bond is quantitatively represented by the value of sign(λ_2)ρ, where a larger (more negative) value indicates a stronger interaction. The distribution patterns in the scatter plots intuitively reveal the nature and strength of hydrogen bonding, providing strong visual corroboration for our previous conclusions [29]. The color scheme in both the RDG scatter plots and the independent gradient model (IGM) isosurfaces denotes specific interaction types: red for steric repulsion, green for van der Waals interactions, and blue for attractive hydrogen bonds. The calculated sign(λ_2)ρ values for the key hydrogen bond in each molecule, in both the S_0 and S_1 states, are displayed in Fig. 3. The observed trend in hydrogen bond strength is: PHL-OH > PHL-NH_2 > PHL-CH_3 > PHL > PHL-CHO > PHL-NO_2 > PHL-CN. This sequence indicates a monotonic decrease in hydrogen bond strength from PHL-OH to PHL-CN. Importantly, the ranking derived from RDG analysis is fully consistent with the trends obtained from geometric parameter analysis (bond lengths and angles), thereby cross-validating the reliability of both methodological approaches.

3.3 Molecular orbital analysis

Molecular orbital analysis elucidates the redistribution of electron density upon excitation, providing a theoretical basis for understanding the correlation between photophysical behavior and chemical reactivity [30, 31]. Given that the excitation characteristics are predominantly governed by the highest occupied molecular orbital (HOMO) to lowest unoccupied molecular orbital (LUMO) transition, we visualized these frontier orbitals. As shown in Fig. 4, the introduction of electron-donating groups (-OH, -NH_2, -CH_3) in PHL-OH, PHL-NH_2, and PHL-CH3 leads to a significant increase in electron density on the proton acceptor oxygen atom (O1). Conversely, for derivatives with electron-withdrawing groups, a marked decrease in electron density on O1 is observed in PHL-CN. Strikingly, in PHL-NO_2 and PHL-CHO, O1 exhibits negligible electron density in the relevant frontier orbital, indicating a severely diminished capacity to accept the proton, which suggests that ESIPT is either highly unfavorable or non-existent in these two derivatives. Therefore, electron-donating groups facilitate the ESIPT process by enhancing electron density on the acceptor site, whereas electron-withdrawing groups effectively inhibit it by depleting this density. Furthermore, in methanol solution, measurable electron density on O1 is present in PHL, PHL-OH, PHL-NH_2, PHL-CH_3, and PHL-CN, confirming their inherent proton-accepting ability. This electron distribution analysis predicts a feasible ESIPT pathway for these five molecules, while strongly indicating its improbability for PHL-NO_2 and PHL-CHO.

3.4 Potential energy curve

To gain deeper mechanistic insight into how substituents regulate the ESIPT process, we computed the potential energy curves (PECs) for phloretin (PHL) and its derivatives in both the S_0 and S_1 states. The energy barrier along the reaction coordinate provides a quantitative measure of the feasibility of ESIPT [32]. Figure 5 presents these PECs, from which the energy barriers were extracted. The intrinsic barrier for pristine PHL in the S_0 state is 4.694 kcal/mol. Introduction of electron-donating groups (-OH, -NH_2, -CH_3) results in slightly lowered barriers of 4.656, 4.682, and 4.690 kcal/mol for PHL-OH, PHL-NH_2, and PHL-CH_3, respectively. Conversely, electron-withdrawing groups (-CN, -NO_2, -CHO) lead to increased barriers of 4.836, 4.834, and 4.702 kcal/mol for PHL-CN, PHL-NO_2, and PHL-CHO. The reduction in barrier height induced by electron-donating groups directly correlates with a decreased difficulty for ESIPT. In contrast, the elevated barriers associated with electron-withdrawing groups indicate a greater thermodynamic impediment to proton transfer. This quantitative trend from PEC analysis is in full agreement with the qualitative predictions derived from geometric, spectroscopic, and orbital analyses discussed above, providing robust and convergent evidence for the substituent effect on ESIPT. Most significantly, the potential energy curve analysis in the S_1 state reveals a critical distinction. For PHL, PHL-OH, PHL-NH_2, PHL-CH_3, and PHL-CN, no energy barrier is present along the proton transfer coordinate in the S_1 state. This barrierless profile indicates that the ESIPT process in these systems is intrinsically more favorable in the excited state than in the S_0 state and can proceed spontaneously from the Franck-Condon (E*) region to the proton-transferred (K*) state. In stark contrast, the derivatives PHL-NO_2 and PHL-CHO exhibit distinct energy barriers of 5.289 and 5.164 kcal/mol, respectively, in the S_1 state. Compared to their S_0 state barriers, these values are significantly higher, implying that ESIPT becomes thermodynamically more difficult or even prohibited upon photoexcitation for these two molecules. These findings demonstrate that introducing electron-donating groups to the PHL scaffold facilitates ESIPT by maintaining or creating a barrierless pathway in S_1, effectively promoting ultrafast proton transfer. Conversely, strong electron-withdrawing groups not only increase the ground-state barrier but also introduce or substantially raise the barrier in the excited state, thereby imposing a significant kinetic hindrance to ESIPT.

3.5 Antioxidant activity

Phloretin, a representative dihydrochalcone, exhibits notable anti-inflammatory and antioxidant properties, making it a promising antioxidant scaffold. To theoretically explore avenues for enhancing its activity, we analyzed the antioxidant potential of PHL and its derivatives. Antioxidant activity is closely correlated with the ionization potential (IP) [33, 34]. According to Koopmans' theorem, a lower IP value corresponds to a greater propensity for electron donation and, consequently, stronger antioxidant activity. The calculated IP values for PHL and its derivatives in both the S_0 and S_1 states are presented in Fig. 6. A key observation is that the antioxidant activity, as gauged by IP, is generally weaker in the S_1 state compared to the S_0 state for these biomolecules. This suggests that to maximize their efficacy as antioxidants, the ESIPT process in PHL-based compounds should be inhibited, preventing their relaxation

into a less active excited-state configuration. Focusing on the ground state (S_0), the introduction of electron-donating groups (-OH, -NH_2, -CH_3) lowers the IP values of PHL-OH, PHL-NH_2, and PHL-CH3 to 6.605, 5.721, and 6.141 eV, respectively. This reduction in IP signifies a significant enhancement in antioxidant activity. Conversely, electron-withdrawing groups (-CN, -NO_2, -CHO) raise the IP values of PHL-CN, PHL-NO_2, and PHL-CHO to 6.489, 6.465, and 6.488 eV, indicating a clear inhibitory effect on antioxidant capacity.

4. Conclusion

This study systematically investigates the regulatory effects of electron-donating and electron-withdrawing groups on the excited-state intramolecular proton transfer (ESIPT) process and the antioxidant activity of phloretin, a representative dihydrochalcone molecule. The key findings are as follows: First, ionization potential calculations reveal that the antioxidant activity in the S_1 state (post-ESIPT) is weaker than in the ground state (S_0), indicating that to preserve antioxidant efficacy, the ESIPT process should be inhibited when these molecules are utilized as antioxidants. Most importantly, potential energy curve analysis shows that derivatives with strong electron-withdrawing groups (-NO_2, -CHO) exhibit significantly higher proton transfer energy barriers in the S_1 state than in the S_0 state, suggesting that ESIPT is unlikely to occur spontaneously in the excited state. In contrast, other molecules display a barrierless proton transfer pathway in the S_1 state. Furthermore, a consistent regulatory trend is established: electron-donating groups simultaneously promote ESIPT and enhance ground-state antioxidant activity, whereas electron-withdrawing groups inhibit ESIPT and reduce antioxidant capacity. The most significant finding of this work lies in revealing the fundamental control that substituents exert over the ESIPT pathway: strong electron-withdrawing groups can construct a kinetic barrier in the excited state, thereby effectively "switching off" the proton transfer channel. This research establishes a theoretical foundation for understanding the structure-activity relationship of dihydrochalcone derivatives and provides clear design principles for synchronously modulating the ESIPT process and antioxidant activity through targeted group modification.

Declarations

Data Availability Statement:

No Data associated in the manuscript

Author Contribution

Z: visualization, writing—original draft. S: supervision. R: soft-ware.A.: conceptualization, project administration. M: resources, materials preparation. B:funding acquisition, W:investigation. All authors have read and agreed to the published version ofthe manuscript.

Acknowledgements

We are grateful to the Xinjiang Natural Science Foundation for General Program (No. 2023D01A40), Research Program of Xinjiang Higher Education (No. XJEDU2023J030), the National Natural Science Foundation of China (No. 22363011), Tianshan Talent Training Program of Xinjiang(No. 2024TSYCCX0064), University of Science and Technology of China- Xinjiang Normal University Counterpart Cooperation and Development Joint Fund（No. XJNULH2503）

References

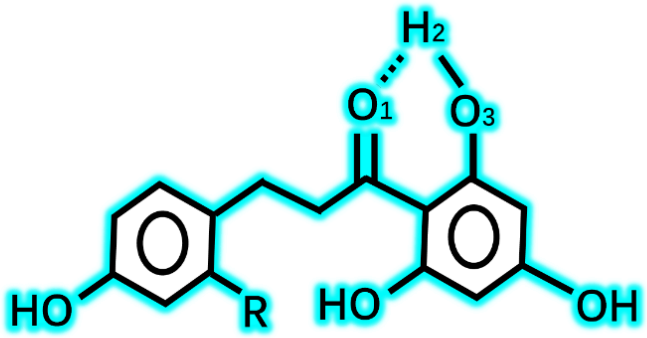
1. Boruah PJ, Venkatesh N, Samanta A, Paul AK (2025). A Theoretical Investigation on the Role of Primary, Secondary, and Tertiary Amine Substituents in Excited State Intramolecular Proton Transfer of p - Amino o - Hydroxy Benzaldehyde. Chemistry-An Asian Journal, 20(21), 12. https://doi.org/10.1002/asia.202500777
2. Cao BF, Li K, Chen CG, Shi Y (2025). Effects of functional groups on ESIPT and antioxidant activity of apigenin : A non-existent enol * state fluorescein. Spectrochimica Acta Part A-Molecular And Biomolecular Spectroscopy, 326, 9. https://doi.org/10.1016/j.saa.2024.125287
3. Chen YH, Sung RB, Sung KG (2018). Insights into Excited State Intramolecular Proton Transfer : An Alternative Model for Excited State Proton Transfer of Green Fluorescence Protein. Journal Of Physical Chemistry A, 122(28), 5931–5944. https://doi.org/10.1021/acs.jpca.8b01799
4. Constantin RP, de Souza MC, Abrahao J, de Paiva Foletto-Felipe M, Grizza LHE, Ferro AP,Marchiosi R (2025). Phytotoxicity and Mode of Action of Phloretin on Maize Seedlings. Journal of Plant Growth Regulation, 44(7), 3916–3936. https://doi.org/10.1007/s00344-025-11673-z
5. Debie E, Kuppens T, Vandyck K, Van der Eycken J, Van Der Veken B, Herrebout W, Bultinck P (2006). Vibrational circular dichroism DFT study on bicyclo[3.3.0]octane derivatives. Tetrahedron-Asymmetry, 17(23), 3203–3218. https://doi.org/10.1016/j.tetasy.2006.11.046
6. Goebel D, Rusch P, Duvinage D, Bigall NC, Nachtsheim BJ (2020). Emission color-tunable oxazol (in) yl-substituted excited-state intramolecular proton transfer (ESIPT)- based luminophores. Chemical Communications, 56(98), 15430–15433. https://doi.org/10.1039/d0cc05780k
7. Hu GX, Guo ML, Li Q, Zhao J, Zhang LY, Yang JY, Shi Y (2025). The substituent effect on the ESIPT and antioxidant activity of dual proton-transfer-site salicylaldehyde azine derivatives. Chemical Physics Letters, 865, 8. https://doi.org/10.1016/j.cplett.2025.141933
8. Hu MR, Li,R Z, Gao SF, Pan H, Luo J (2026). Photophysical properties of 5-methoxyflavone and its protonated species influenced by intermolecular hydrogen bonding and environmental rigidity. Dyes And Pigments, 245, 7. https://doi.org/10.1016/j.dyepig.2025.113269
9. Ichikawa K, Sasada R, Chiba K, Gotoh H (2019). Effect of Side Chain Functional Groups on the DPPH Radical Scavenging Activity of Bisabolane-Type Phenols. Antioxidants, 8(3), 11. https://doi.org/10.3390/antiox8030065

10. Ji FX, Guo YR, Wang MQ, Wang C, Wu ZB, Wang SP, Zhao GJ (2021). New insights into ESIPT mechanism of three sunscreen compounds in solution : A combined experimental and theoretical study. Colloids And Surfaces B-Biointerfaces, 207, 7. https://doi.org/10.1016/j.colsurfb.2021.112039
11. Kayikci M, Venkatakrishnan AJ, Scott-Brown J, Ravarani CNJ, Flock T, Babu MM (2018). Visualization and analysis of non-covalent contacts using the Protein Contacts Atlas. Nature Structural & Molecular Biology, 25(2), 185. https://doi.org/10.1038/s41594-017-0019-z
12. Lee CY, Sharma A, Semenya J, Anamoah C, Chapman KN, Barone V (2020). Computational Study of Ortho - Substituent Effects on Antioxidant Activities of Phenolic Dendritic Antioxidants. Antioxidants, 9(3), 14. https://doi.org/10.3390/antiox9030189
13. Li MT, Yang XY, Zhao MC, Shang CJ, Wang DD, Li JJ, Wang LL (2023). Effects of carboxyl - and amino-groups on the antioxidant activity of hydroxyanthraquinones with ESIPT property : A theoretical study. Journal of Molecular Liquids, 376, 10. https://doi.org/10.1016/j.molliq.2023.121497
14. Li Y, Liu XC, Han JH, Cao BF, Sun CF, Diao LH, Shi Y (2019). Solvent viscosity induces twisted intramolecular charge transfer state lifetime tunable of Thioflavin-T. Spectrochimica Acta Part A-Molecular And Biomolecular Spectroscopy, 222, 7. https://doi.org/10.1016/j.saa.2019.117244
15. Lu T (2024). A comprehensive electron wavefunction analysis toolbox for chemists, Multiwfn. Journal of Chemical Physics, 161(8), 41. https://doi.org/10.1063/5.0216272
16. Lu T, Chen FW (2012). Multiwfn: A multifunctional wavefunction analyzer. Journal of Computational Chemistry, 33(5), 580–592. https://doi.org/10.1002/jcc.22885
17. Prutskij T, Deriabina A, Leon GDV, Trejo LC (2024). Excited-state proton transfer based fluorescence in Kaempferol powder and solutions with different concentrations. Spectrochimica Acta Part A-Molecular And Biomolecular Spectroscopy, 309, 7. https://doi.org/10.1016/j.saa.2023.123814
18. Sharma S, Ghosh KS (2021). Recent advances (2017–20) in the detection of copper ion by using fluorescence sensors working through transfer of photo-induced electron (PET), excited-state intramolecular proton (ESIPT) and Forster resonance energy (FRET). Spectrochimica Acta Part A-Molecular And Biomolecular Spectroscopy, 254, 18. https://doi.org/10.1016/j.saa.2021.119610
19. Shen N, Wang TF, Gan Q, Liu S, Wang L, Jin B (2022). Plant flavonoids : Classification, distribution, biosynthesis, and antioxidant activity. Food Chemistry, 383, 13. https://doi.org/10.1016/j.foodchem.2022.132531
20. Sonika S, Dhiman S, Singh AS, Luxami V, Kumar G (2025). Excited-state relaxation mechanisms of Janus-type proton in benzimidazole-conjugated aminomaleonitrile : single or double proton transfer? *Physical Chemistry Chemical Physics*, 27(28), 14976–14984. https://doi.org/10.1039/d5cp01412c
21. Tang XZ, Wang LL, Zhang YJ, Sun CF (2025a). Relationship between antioxidant activity and ESIPT process based on flavonoid derivatives : A comprehensive analysis. Spectrochimica Acta Part A-Molecular And Biomolecular Spectroscopy, 327, 10. https://doi.org/10.1016/j.saa.2024.125370

22. Tang XZ, Wang LL, Zhang YJ, Sun CF (2025b). Relationship between antioxidant activity and ESIPT process based on flavonoid derivatives : A comprehensive analysis. Spectrochimica Acta Part A-Molecular And Biomolecular Spectroscopy, 327, 10. https://doi.org/10.1016/j.saa.2024.125370
23. Tao YP, Zhang HW, Wang Y (2023). Revealing and predicting the relationship between the molecular structure and antioxidant activity of flavonoids. Lwt-Food Science And Technology, 174, 7. https://doi.org/10.1016/j.lwt.2023.114433
24. Tian CL, Liu X, Chang Y, Wang RX, Lv TM, Cui CC, Liu MC (2021). Investigation of the anti-inflammatory and antioxidant activities of luteolin, kaempferol, apigenin and quercetin. South African Journal of Botany, 137, 257–264. https://doi.org/10.1016/j.sajb.2020.10.022
25. Wang JW, Zhao YY, Zhai BT, Cheng JX, Sun J, Zhang XF, Guo DY (2023). Phloretin Transfersomes for Transdermal Delivery : Design, Optimization, and In Vivo Evaluation. Molecules, 28(19), 19. https://doi.org/10.3390/molecules28196790
26. Xiao YL, Shen JF, Zhan JF, Guo LM, Ho CT, Li SM (2024). Antiglycating effects of citrus flavonoids and associated mechanisms. Food Science And Human Wellness, 13(5), 2363–2372. https://doi.org/10.26599/FSHW.2022.9250247
27. Yang DP, Yang YG(2024). Theoretical insights into excited state behaviors of D3HF derivatives via altering atomic electronegativity of chalcogen. Spectrochimica Acta Part A-Molecular And Biomolecular Spectroscopy, 313, 8. https://doi.org/10.1016/j.saa.2024.123926
28. Yin CM, Duan YN, Xiang L, Wang GS, Zhang XF, Shen, X.,... Mao, Z. (2018). Effects of phloridzin, phloretin and benzoic acid at the concentrations measured in soil on the root proteome of Malus hupehensis Rehd Seedlings. *SCIENTIA HORTICULTURAE*, 228, 10–17. https://doi.org/10.1016/j.scienta.2017.09.044
29. Zhang C, Zhao Y, Tao H, Li LY, He YQ, Zhang XY, Hong GJ (2023). Analysis of the Flavonoidome Reveals the Different Health-Promoting Flavonoid Characteristics in Fruit. Antioxidants, 12(9), 13. https://doi.org/10.3390/antiox12091665
30. Zhang YS, Xia N, Ding ZZ, Song JJ, Zhang YN, Li CX, Feng ZS (2025). Preparation, structural changes and functional properties of the covalent complexes of almond protein and phloretin. International Journal of Biological Macromolecules, 293, 13. https://doi.org/10.1016/j.ijbiomac.2024.139322
31. Zhang ZY, Fang H (2024). Regulating fluorescent properties and ESIPT behavior of novel flavone-based fluorophore by replacing oxygen atom in proton donor / acceptor with sulfur atom : A TD-DFT study. Journal of Luminescence, 265, 9. https://doi.org/10.1016/j.jlumin.2023.120209
32. Zhao GJ, Shi W, Yang, YF, Ding Y, Li YQ (2021). Substituent Effects on Excited-State Intramolecular Proton Transfer Reaction of 2-Aryloxazoline Derivatives. Journal of Physical Chemistry A, 125(13), 2743–2750. https://doi.org/10.1021/acs.jpca.0c10799
33. Zhao GJ, Han KL (2012). Hydrogen Bonding in the Electronic Excited State. Accounts Of Chemical Research, 45(3), 404–413. https://doi.org/10.1021/ar200135h
34. Zheng YZ, Chen DF, Deng G, Guo R, Fu ZM (2018). The antioxidative activity of piceatannol and its different derivatives : Antioxidative mechanism analysis. Phytochemistry, 156, 184–192.

https://doi.org/10.1016/j.phytochem.2018.10.004

Figures



Name of derivative	Substituent
PHL	R=H
PHL-OH	R=OH
PHL-NH_2	R=NH_2
PHL-CH_3	R=CH_3
PHL-CN	R=CN
PHL-NO_2	R=NO_2
PHL-CHO	R=CHO

Figure 1

Molecular structure of phloretin and its derivatives

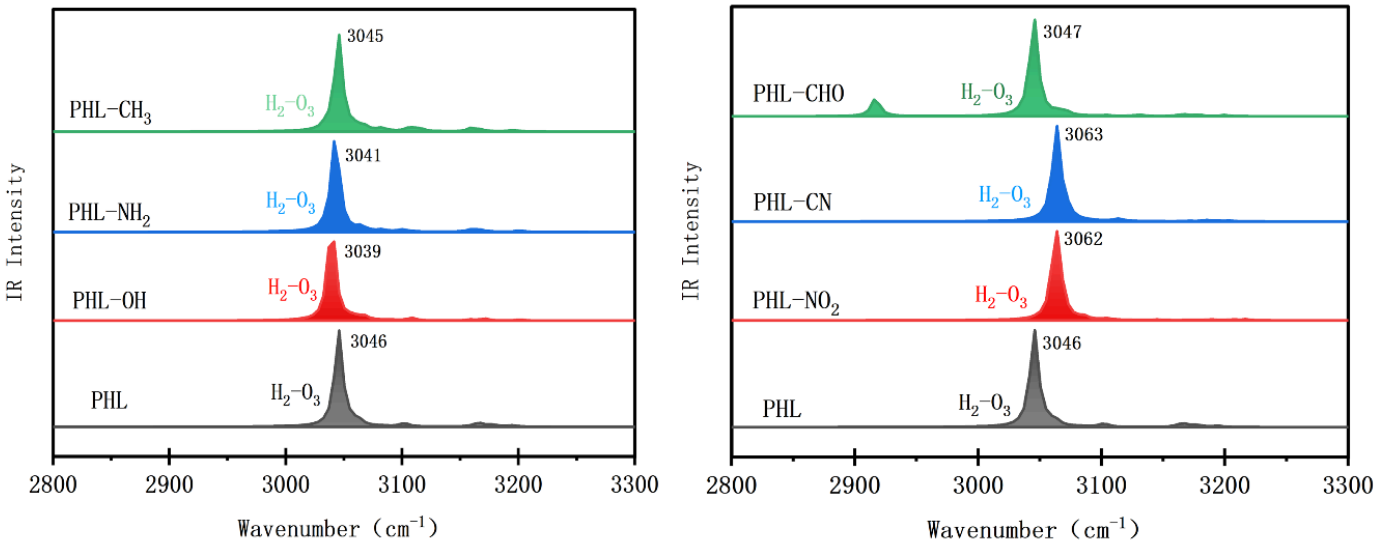


Figure 2

Calculated O–H Stretching Frequencies and Intensities for Phloretin (PHL) and Its Derivatives in Methanol, Reflecting Intramolecular Hydrogen Bond (O1–H2···O3) Strength.

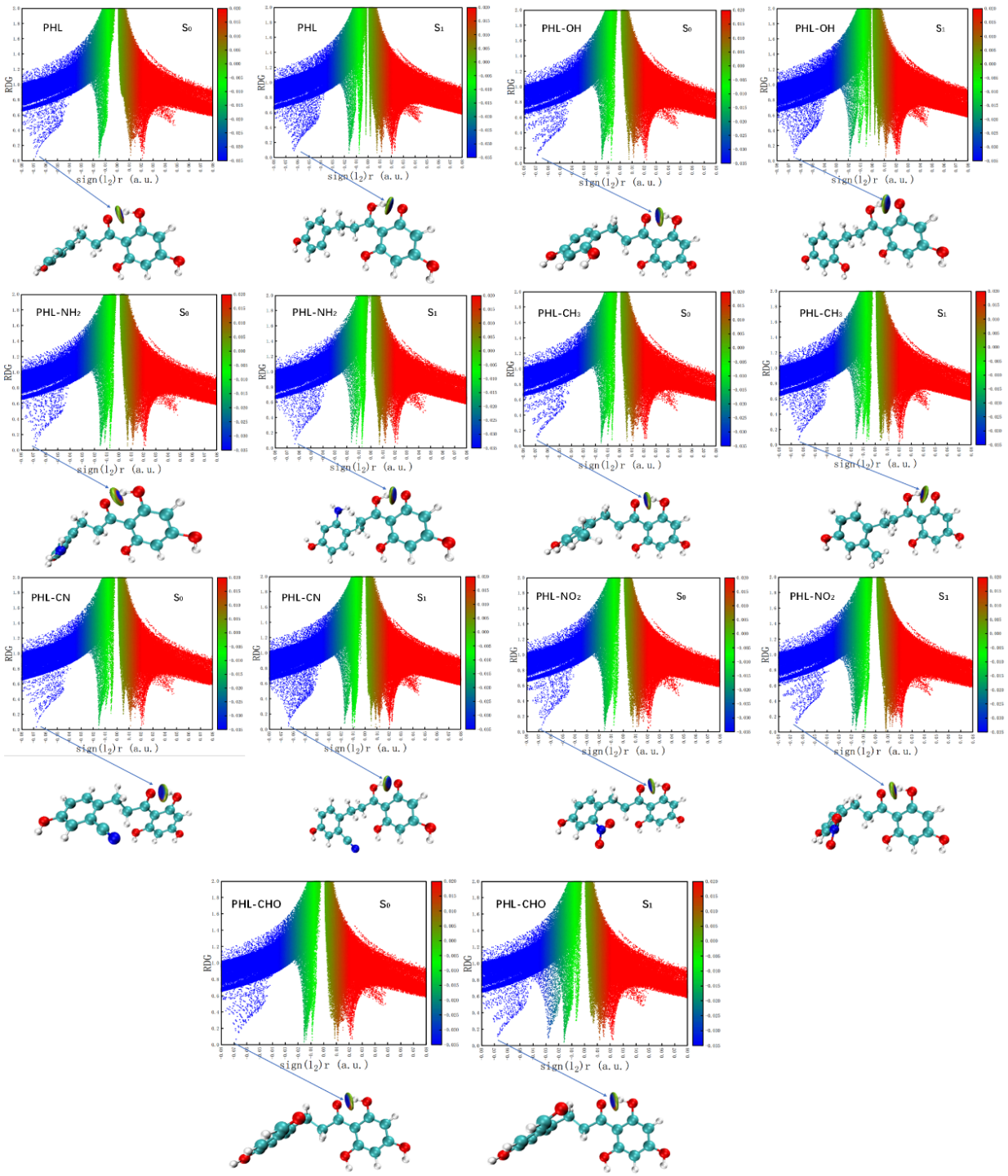


Figure 3

NCI scatter plots of PHL molecules and their derivatives in S0 state and S1 state.

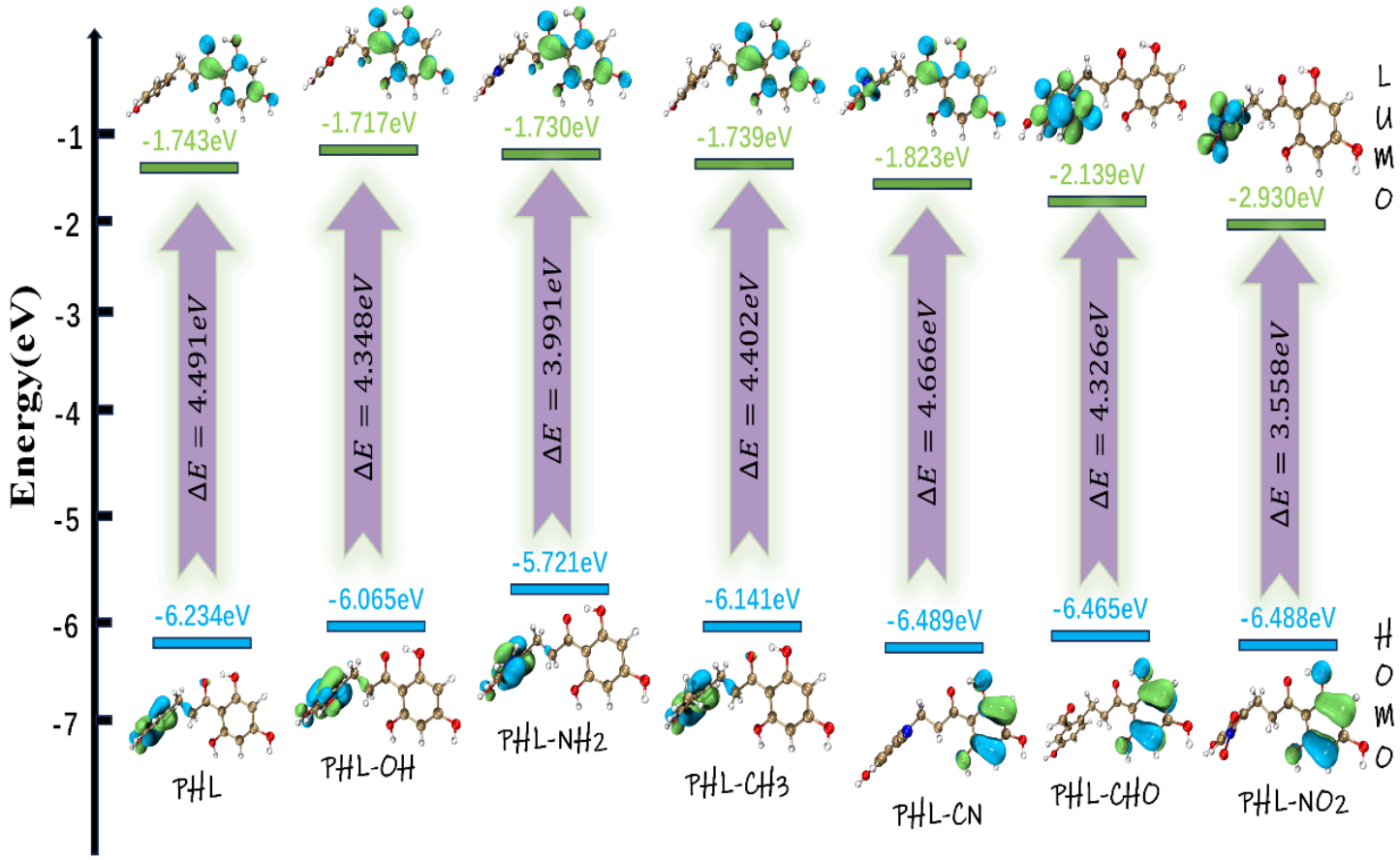


Figure 4

Frontier molecular orbitals (HOMO and LUMO) of phloretin and its derivatives in methanol solution.

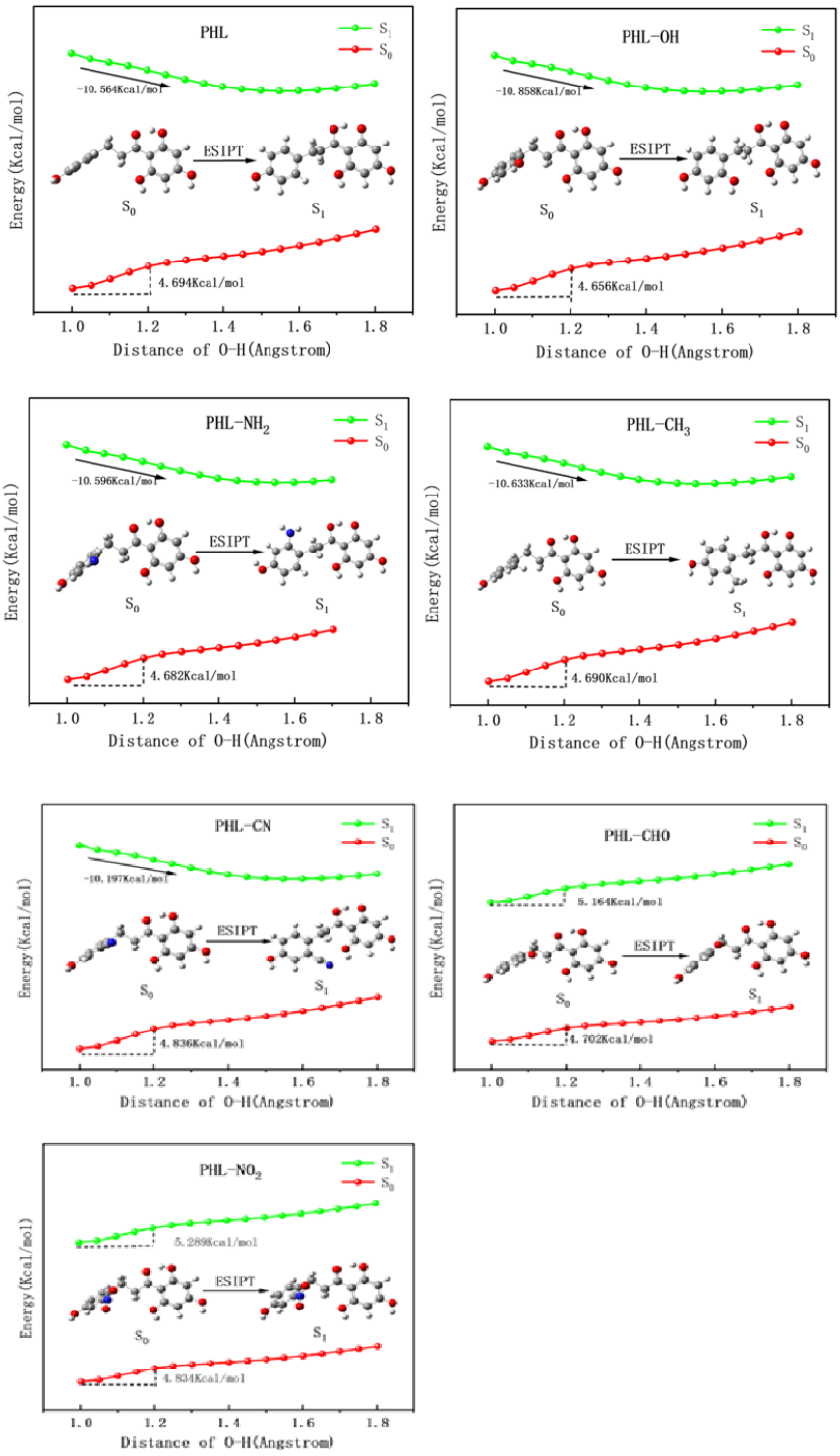


Figure 5

Potential energy curves of PHL molecule and its derivatives in methanol solution

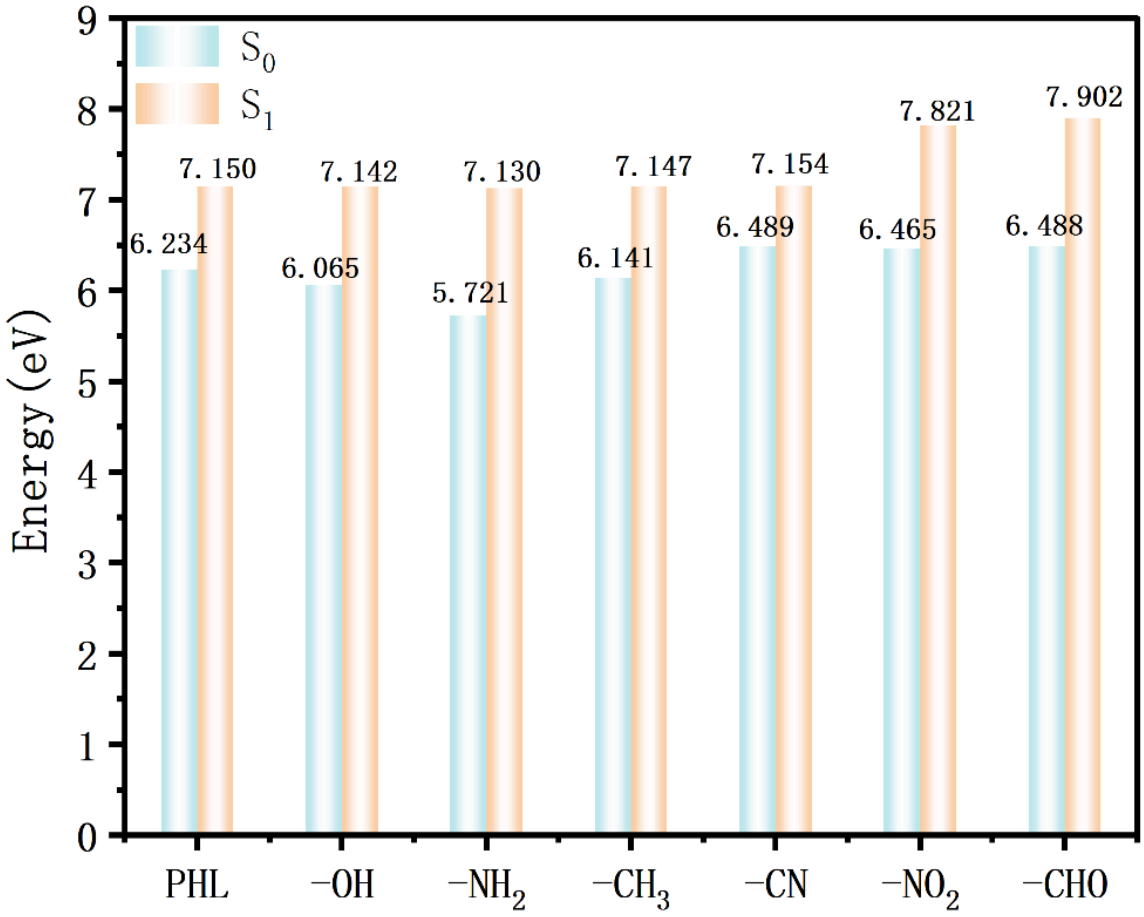


Figure 6

Ionization potentials (IP) of phloretin and its derivatives in the S_0 and S_1 states.